Analysis of lacrimal duct morphology from cone-beam CT dacryocystography in a Japanese population

Jutaro Nakamura (jutaro_n@yokohama-cu.ac.jp)
Department of Ophthalmology and Visual Science, Yokohama City University Graduate School of Medicine

Tomoyuki Kamao
Department of Ophthalmology, Ehime University Graduate School of Medicine

Arisa Mitani
Department of Ophthalmology, Ehime University Graduate School of Medicine

Nobuhisa Mizuki
Department of Ophthalmology and Visual Science, Yokohama City University Graduate School of Medicine

Atsushi Shiraishi
Department of Ophthalmology, Ehime University Graduate School of Medicine

Research Article

Keywords: Dacryocystography, Cone-beam computed tomography, Dacryoendoscope, Primary acquired nasolacrimal duct obstruction, Endoscopic-assisted nasolacrimal duct intubation

Posted Date: December 6th, 2021

DOI: https://doi.org/10.21203/rs.3.rs-1137390/v1

Abstract

Dacryocystorhinostomy (DCR) is the first-line treatment for lacrimal duct stenosis and obstruction in western countries. Endoscopic-assisted nasolacrimal duct intubation (ENDI) is spreading steadily as a minimally invasive treatment in Northeast Asia. ENDI is prevalent in this area because Northeast Asians have relatively flat facial features, with a less elevated superior orbital rim than other ethnic groups. This allows for relatively easy manipulation of a dacryoendoscope. Evidence has accumulated that the morphology and inclination of the lacrimal duct differ among individuals and ethnic groups. In this study, we collected anthropometric data from a Japanese population of 100 samples—the parameters vital for designing a dacryoendoscope probe. The data we provided was essential in designing the overall length, bending point, and curve-line of the dacryoendoscope probe. Although the Japanese data measured in this study would not be directly applicable to other ethnic groups, we hope that the parameters provided by this study will contribute to the accumulation of valuable anthropometric data for the design of endoscopic probe morphologies and the development of therapeutic devices for lacrimal tract diseases—in terms of designing optimal morphologies, specific to ethnic groups and populations.

Introduction

The lacrimal duct extends from the lacrimal punctum to the lower opening of the nasolacrimal duct (NLD) on the lateral wall of the inferior nasal meatus. It passes through upper and lower punctum, the superior and inferior canaliculi, and the common canaliculus to reach the internal common punctum (ICP) in the lacrimal sac. The pathway to this point passes through eyelid tissue that is mobile and elastic. The lacrimal sac (LS) is located in the lacrimal fossa. The interosseous and meatal parts of the NLD are fixed tissues.

Primary acquired nasolacrimal duct obstruction (PANDO) is an organic obstruction of the lacrimal duct that can occur anywhere from the punctum to the NLD opening.[1] Cases with obstruction from the punctum to the ICP are classified as *lacrimal canaliculus obstruction*, while cases with obstruction from the LS to the NLD opening are classified as *nasolacrimal duct obstruction*. Dacryocystorhinostomy (DCR) is the first-line treatment for PANDO. Endoscopic-assisted nasolacrimal duct intubation (ENDI) is widely used as a minimally invasive treatment for lacrimal duct stenosis and obstruction in Northeast Asia.[2–5] The ENDI procedure is performed while directly observing the obstructed area in the lacrimal duct with a dacryoendoscope and observing the nasal cavity with a nasal endoscope. This reduces complications from false passage formation. Because ENDI can usually be performed under local anesthesia, it has evolved into a less invasive and safer procedure, which is one of the main reasons for its increasingly widespread use in Northeast Asia. Another reason is that Northeast Asians have relatively flat facial features, with a less elevated superior orbital rim (SOR) than other ethnic groups. This allows for relatively easy manipulation of a dacryoendoscope.[6] In general, the long-term therapeutic outcomes of ENDI are not equivalent to DCR. Nevertheless, evidence has accumulated that the outcomes of ENDI are almost as effectual as DCR for canaliculus obstruction and PANDO (in cases of non-inflammatory or partial obstruction).[2,4,5,7–9] Since ENDI is a minimally invasive procedure for the treatment of PANDO, which can

be performed under local anesthesia, further studies are needed to compare the long-term treatment outcomes of DCR and ENDI in PANDO, in terms of pathological conditions (e.g., site of obstruction, cause of obstruction, and duration of obstruction).

Since it was first reported in 1909, dacryocystography (DCG) has undergone improvements in contrast media, injection method (using a cannula), and imaging method. DCG is still an essential preoperative evaluation for PANDO.[10,11]

Since its first application in dentistry in 1998, clinical applications of cone-beam computed tomography (CBCT) have gradually increased in the head and neck regions; CBCT is now widely used in medical facilities for dentistry, oral surgery, and otorhinolaryngology.[12–15] There are few reports on CBCT in the field of ophthalmology. Nonetheless, CBCT-DCG is a valuable test for evaluating PANDO. It has the advantage of much lower radiation exposure than conventional multi-slice CT-DCG.[16–18]

The length and inclination of the LS and NLD differ among individuals; there are also differences between races and ethnic groups. This is the first study to report measurements of various parameters of the lacrimal duct in a Japanese population, based on CBCT-DCG. We hope that the measurements provided by this study will contribute to the accumulation of valuable anthropometric data for the design of endoscopic probe morphologies and the development of therapeutic devices for lacrimal tract diseases (in terms of designing optimal morphologies, specific to ethnic groups and populations).

Results

The mean age of the 102 cases was 71.3 ± 11.7 years. Among them, 74 cases were female and 28 cases were male. There were 51 cases of right side PANDO and 51 cases of left-side PANDO. The maximum, minimum, and average values of the measured parameters are shown in Table 1.

Table 1
Various lacrimal duct parameters measured from sagittal section CBCT-DCG images

	1	2	3	4	5	6
Parameters	**SOR–ICP–NLD opening angle**	**SOR–ICP length**	**ICP–NLD opening length**	**LS length**	**NLD length**	**LS–NLD angle**
Description	Angle formed by the superior orbital rim, internal common punctum, and nasolacrimal duct opening	Length from the superior orbital rim to the internal common punctum	Length from the internal common punctum to the nasolacrimal duct opening	Length from the internal common punctum to the transition	Length from the transition to the nasolacrimal duct opening	Angle formed by the lacrimal sac and the nasolacrimal duct
Mean value	10.2±7.8°	24.3±3.2 mm	21.8 ± 2.7 mm	8.9 ± 2.3 mm	13.2 ± 2.7 mm	−6.3 ± 14.1°
Maximum value	27°	32.2 mm	30.5 mm	17.1 mm	20.7 mm	40°
Minimum value	−11°	10.8 mm	14.2 mm	4.3 mm	5.7 mm	−43°
p-**value**[*1]	0.5528	0.0163	0.039	0.0002	0.3946	0.3007
Normal distribution	YES	NO	NO	NO	YES	YES
Mean values of the females	9.9 ± 8.2°	23.9 ± 3.2 mm	21.3 ± 2.5 mm	8.7 ± 2.1 mm	13.0 ± 2.4 mm	−6.9 ± 14.5°
Mean values of the males	10.8 ± 6.7°	25.2 ± 3.1 mm	23.2 ± 2.7 mm	9.6 ± 2.6 mm	13.7 ± 3.3 mm	−4.6 ± 12.9°
p-**value**[*2]	0.6706	0.0746	0.0014	0.0785	0.1723	0.2862
Sexual difference	NO	NO	YES	NO	NO	NO

Note: *[1] The *p*-value in the normal distribution column was calculated by the Shapiro–Wilk test; $p > 0.05$ indicated that the distribution was normal. *[2], The non-parametric Mann–Whitney U test was used to compare the two groups of females and males. The results were considered significant at a *p*-value of < 0.05.

Abbreviations: SOR, superior orbital rim; NLD, nasolacrimal duct; ICP, internal common punctum; LS, lacrimal sac.

The angle formed by SOR–ICP–NLD opening

The maximum value of the angle was 27° and the minimum value was −11°. The mean value was 10.2 ± 7.8°. The angle was positive in 92% (93/101) of cases, while 8% (8/101) of the subjects had a negative angle. An example image of a case with a large SOR–ICP–NLD opening angle is shown in Fig. 3. The large angle was due to the elevation of the SOR and anterior inclination of the NLD. The Shapiro–Wilk test gave a value of 0.55, indicating a normal distribution (Fig. 4A). For females, the mean was 9.9 ± 8.2°; for males, it was 10.8 ± 6.7°. There was no significant difference between males and females (p = 0.67).

The length of SOR–ICP

The maximum and minimum lengths were 32.2 mm and 10.8 mm, respectively. The mean was 24.3 ± 3.2 mm; the Shapiro–Wilk test gave a value of 0.016, indicating a non-normal distribution (Fig. 4B). For females, the mean was 23.9 ± 3.2 mm; for males, it was 25.2 ± 3.1 mm. There was no significant difference between males and females (p = 0.07).

The length of ICP–NLD opening

The maximum and minimum lengths were 30.5 mm and 14.2 mm, respectively. The mean was 21.8 ± 2.7 mm. The Shapiro–Wilk test gave a value of 0.039, indicating a non-normal distribution (Fig. 4C). For females, the mean was 21.3 ± 2.5 mm; for males, it was 23.2 ± 2.7 mm. There was a significant difference between males and females (p = 0.0014).

The length of LS

The maximum value was 17.1 mm and the minimum value was 4.3 mm. The mean was 8.9 ± 2.3 mm. The Shapiro–Wilk test gave a value of 0.0002, indicating a non-normal distribution (Fig. 4D). For females, the mean was 8.7 ± 2.1 mm; for males, it was 9.6 ± 2.6 mm. There was no significant difference between females and males (p = 0.079).

The length of NLD

The maximum value was 20.7 mm and the minimum value was 5.7 mm. The mean was 13.2 ± 2.7 mm. The Shapiro–Wilk test gave a value of 0.39, showing a normal distribution (Fig. 4E). For females, the mean was 13.0 ± 2.4 mm; for males, it was 13.7 ± 3.3 mm. There was no significant difference between females and males (p = 0.17).

The LS–NLD angle

The maximum angle was 40° and the minimum was −43°. The mean was −6.3 ± 14.1°. The Shapiro–Wilk test gave a value of 0.30, indicating a normal distribution (Fig. 4F). The anterior bending type represented 33.3% (31/93) of cases; 66.7% (62/93) were of the posterior bending type. Examples of cases with anterior

and posterior bending are shown in Figs. 5 and 6. For females, the mean was −6.9 ± 14.5°; for males, it was −4.6 ± 12.9°. There was no significant difference between males and females (p = 0.29).

Discussion

The lengths of the LS and the NLD and the inclination of the LS–NLD vary among individuals and between ethnic groups.[19–23] In this study, we measured various parameters of the Japanese lacrimal duct using CBCT-DCG images.

The average angle formed by the SOR–ICP–NLD opening was 10.2 ± 7.8°. The line formed by the SOR–ICP is the anatomical limit where the tip of a straight probe can reach most anteriorly after entering the NLD through the ICP. We confirmed that, in 92% of subjects, the line formed by the ICP–NLD opening was anteriorly inclined to the line formed by the SOR–ICP. This suggests that blind probing with a straight bougie, or manipulating a dacryoendoscope with a straight probe, is more likely to form a false passage posterior to the original lacrimal duct. Therefore, a probe with a bent anterior tip, or a curved probe, is more appropriate. In 8% of the subjects, the SOR–ICP–NLD angle was zero or negative. In such cases, a straight probe is considered more suitable than a curved one.

The mean length of the SOR–ICP was 24.3 ± 3.2 mm. The mean length of the ICP–NLD opening was 21.8 ± 2.7 mm. These new parameters could be measured because CBCT-DCG depicts the ICP. Although these parameters did not follow a normal distribution, they may be helpful for optimizing the length and the curve line settings of the dacryoendoscope probe. Generally, Northeast Asians have a low development of the SOR and a relatively flat facial appearance. The angles and lengths in other ethnic groups that have a well-developed SOR may be different from our study's results. By measuring the angles and lengths of several other races and ethnic groups, it will be possible to develop dacryoendoscope probes that are more suitable for the anthropometric structure of the target population.

Based on anatomical measurements in Japanese cadavers, the average length from the lacrimal punctum to the ICP is 11 mm. The average axial length of the LS is 12–15 mm, with the average diameter being 3 mm (the lumen was 1–2 mm). The average length of the NLD is 12–17 mm.[21,24]

In our study, the length from the ICP to the LS–NLD transition was 8.9 ± 2.3 mm; the length from the LS–NLD transition to the NLD opening was 13.2 ± 2.7 mm. In fact, as the length from the ICP to the LS–NLD transition refers to the length of the LS body, the actual axial length of the LS can be assumed to be 2–3 mm longer—the length of the fundus of the LS. It was challenging to measure the total length of the LS because the contrast medium had already flowed out of the LS at the time of imaging. Thus, the fundus of the LS was often poorly visualized. Therefore, we measured the distance between the ICP and the LS–NLD transition, which was clearly delineated. The distance from the LS–NLD transition to the NLD opening was, in fact, the length of the bony nasolacrimal canal. The interosseous part of the NLD does not have an entirely linear structure but sometimes has a complicated and diverse curvature. Therefore, our measurements do not represent the actual length of the NLD. We acknowledge the necessity of developing a more accurate method for evaluating the length of the NLD.

Several studies have investigated the LS–NLD angle. We found a mean LS–NLD angle of −6.3 ± 14.1° (range, −43° to +40°). The average angle of the anterior bending type (33.3% of cases) was 8.8 ± 14.1°; that of the posterior bending type (66.7% of cases) was −13.8 ± 13.3°. In an anatomical survey of Japanese cadavers, Narioka et al. reported that the anterior bending type accounted for 80% of cases, with an average angle of +8.9 ± 5.0° (range, 0°–19°), and the posteriorly-bending type accounted for 20% of cases, with an average angle of −12.3 ± 9.0° (range, −2° to −26°).[25] By contrast, Park et al. reported that the mean LS–NLD angle was −10.3° and that about 90% of cases were posterior bending.[26] Our data was provided by a larger number of cases and was normally distributed. For more accurate values, it is necessary to increase the number of measurements and to accumulate data on the LS–NLD angle and the frequencies of anterior and posterior bending variations.

There are several limitations to this study. First, we did not evaluate normal lacrimal duct morphology; we evaluated the contralateral lacrimal duct of patients diagnosed with unilateral PANDO. We cannot exclude the possibility that a unilateral PANDO case in this study might develop into a bilateral PANDO case. Second, our measurements were obtained from two-dimensional images; in essence, we need to obtain measurements in three dimensions. It has been reported that, in coronal section, the LS is inclined laterally to the midline and the NLD is inclined medially to the LS. Approximately one-third of the NLD is medially inclined, and two-thirds are laterally inclined, relative to the midline.[25] Furthermore, the NLD does have a linear structure but bends in complicated and diverse ways. Although we used planimetric data in sagittal section, the actual lengths of LS and NLD (and their constituent angles) should be represented in three dimensions. In future research to evaluate the parameters of the lacrimal duct, DCG images should be converted into three dimensions.

Methods

Patient selection

The subjects of this study were patients diagnosed with unilateral PANDO at Ehime University Hospital from December 2015 to April 2021. Diagnosis was obtained through the irrigation test, dacryoendoscopic examination, and CBCT-DCG. We retrospectively analyzed the CBCT-DCG images of the contralateral side of 102 cases diagnosed with unilateral PANDO. There were no abnormalities on the contralateral side in all the above tests. A typical example of a CBCT-DCG image, sectioning the lacrimal duct, is shown in Fig. 1. The patient had been diagnosed with left-sided unilateral PANDO. Fig. 1 shows a DCG image of the right side, contralateral to the obstructed side.

In CBCT-DCG images of a sagittal section, the following parameters were evaluated: 1) the angle formed by SOR–ICP–NLD opening (Fig. 2A); 2) The length of SOR–ICP (Fig. 2B); and 3) The length of ICP–NLD opening (Fig. 2B). To measure these parameters, the following method was applied. A straight line starting from the ICP was drawn in the direction of the SOR; the tangent point on the SOR was determined. The distal end of the interosseous NLD was defined as the NLD opening. The angle formed by the line connecting the tangent point of SOR–ICP and the line connecting ICP–NLD opening was measured.

Next, the following parameters were measured: 4) the length of LS (Fig. 2C); 5) the length of NLD (Figure 2C); and 6) the angle formed by LS–NLD (Fig. 2D). The LS–NLD transition was determined by the sagittal projection of the area corresponding to the origin of the interosseous NLD in the horizontal section of the CBCT image. Of the above, parameter 4 refers to the length from the LS–NLD transition to the ICP, parameter 5 refers to the length from the LS–NLD transition to the NLD opening, and parameter 6 refers to the angle formed by a line connecting the ICP–LS and a line connecting the LS–NLD transition–NLD opening. In the anterior bending type, the angles were designated by plus values, and in the posterior bending type, the angles were shown by negative values.

DCG and CBCT procedures

After topical anesthesia with 4% lidocaine instillation, a 23-gage curved lacrimal cannula was inserted into the upper and lower punctum. A nonionic, water-soluble contrast agent (1–2 ml; Omnipaque 300® [iohexol]; GE Healthcare, Tokyo, Japan) was manually injected slowly until the patient reported the solution reaching the nasal antrum, or until the contrast agent flowed back from the punctum. CBCT imaging was performed within 10 minutes after injection of the contrast medium. CBCT images were acquired using a 3D Accuitomo F17 (Morita, Kyoto, Japan). The imaging conditions were: scan time, 17.5 seconds; X-ray output, 90 kV and 8.0 mA. The length and angle measurements from the images were made using dedicated computer software (i-Dixel 2.0; Morita, Kyoto, Japan). The images were converted to monochrome to facilitate observation of the contrast media.

Statistical analysis

Data were analyzed using JMP software ver. 11.2 (SAS Institute, Cary, NC, USA). The Shapiro–Wilk test was used to determine whether measurement data followed a normal distribution; a p-value of >0.05 was considered to indicate normality in the distribution. The Mann–Whitney U test was used to test the significance of differences for each parameter between males and females. A p-value of <0.05 was considered significant.

Declarations

Ethical approval and consent to participate

This study and its data collection protocol were approved by the Institutional Review Board of Ehime University (Ethical Approval Number: 1601003). The study was registered with the University Hospital Medical Information Network Clinical Trials Registry (Number: UMIN 000025180). Written informed consent was obtained from each patient before enrollment. All procedures used in this study were performed in accordance with the tenets of the Declaration of Helsinki.

Acknowledgements

This study was supported by the Japan Society for the Promotion of Science (JSPS) Postdoctoral Fellowship for Research Abroad (Kaitoku-NIH, #24112 to JN). The funding source had no role in the study design, data collection, and analysis, decision to publish, or preparation of the manuscript.

Conflict of interest

The authors declare that they have no competing interests. The authors alone are responsible for the content and writing of the paper.

Author Contributions

JN contributed for conception, data extraction, analysis, and drafting. TK worked for the surgical operations, data extraction, interpretation of the results and drafting. AM and AS contributed for the surgical operations, data acquisition, and interpretation of the results. TK, AM and AS provided statistical advice. NM and AS provided general management of the study. NM and AS critically revised the protocol and main manuscript.

Data availability

The datasets analyzed during the current study are available from the corresponding author (JN) on reasonable requests.

References

1. Mandeville, J. T. & Woog, J. J. Obstruction of the lacrimal drainage system. *Curr Opin Ophthalmol*, **13**, 303–309 https://doi.org/doi:10.1097/00055735-200210000-00003 (2002).
2. Javate, R. M., Pamintuan, F. G. & Cruz, R. T. Jr. Efficacy of endoscopic lacrimal duct recanalization using microendoscope. *Ophthalmic Plast Reconstr Surg*, **26**, 330–333 https://doi.org/doi:10.1097/IOP.0b013e3181c7577a (2010).
3. Kamao, T., Takahashi, N., Zheng, X. & Shiraishi, A. Changes of Visual Symptoms and Functions in Patients with and without Dry Eye after Lacrimal Passage Obstruction Treatment. *Curr Eye Res*, 1–8 https://doi.org/doi:10.1080/02713683.2020.1760305 (2020).
4. Kamao, T., Zheng, X. & Shiraishi, A. Outcomes of bicanalicular nasal stent inserted by sheath-guided dacryoendoscope in patients with lacrimal passage obstruction: a retrospective observational study. *BMC Ophthalmol*, **21**, 103 https://doi.org/doi:10.1186/s12886-020-01678-5 (2021).
5. Lee, S. M. & Lew, H. Transcanalicular endoscopic dacryoplasty in patients with primary acquired nasolacrimal duct obstruction. *Graefes Arch Clin Exp Ophthalmol*, **259**, 173–180 https://doi.org/doi:10.1007/s00417-020-04833-2 (2021).
6. Whitnall, S. E. Anatomy of the Human Orbit and Accessory Organs of Vision. *Krieger Publishing, Huntington, NY* (1979)
7. Matsumura, N. *et al.* Transcanalicular endoscopic primary dacryoplasty for congenital nasolacrimal duct obstruction. *Eye (Lond)*, **33**, 1008–1013 https://doi.org/doi:10.1038/s41433-019-0374-6 (2019).
8. Mimura, M., Ueki, M., Oku, H., Sato, B. & Ikeda, T. Indications for and effects of Nunchaku-style silicone tube intubation for primary acquired lacrimal drainage obstruction. *Jpn J Ophthalmol*, **59**, 266–272 https://doi.org/doi:10.1007/s10384-015-0381-5 (2015).

9. Sugimoto, M. & Inoue, Y. Long-term Outcome of Dacryoendoscope-assisted Intubation for Nasolacrimal Duct Obstruction. *Journal of the eye*, **27** (9), 1291–1294 (2010).
10. Montecalvo, R. M. *et al.* Evaluation of the lacrimal apparatus with digital subtraction macrodacryocystography., **10**, 483–490 https://doi.org/doi:10.1148/radiographics.10.3.2188309 (1990).
11. Singh, S., Ali, M. J., Paulsen, F. & Dacryocystography From theory to current practice. *Annals of Anatomy - Anatomischer Anzeiger*, **224**, 33–40 https://doi.org/doi:10.1016/j.aanat.2019.03.009 (2019).
12. Cakli, H. *et al.* Use of cone beam computed tomography in otolaryngologic treatments. *Eur Arch Otorhinolaryngol*, **269**, 711–720 https://doi.org/doi:10.1007/s00405-011-1781-x (2012).
13. Mozzo, P., Procacci, C., Tacconi, A., Martini, P. T. & Andreis, I. A. A new volumetric CT machine for dental imaging based on the cone-beam technique: preliminary results. *Eur Radiol*, **8**, 1558–1564 https://doi.org/doi:10.1007/s003300050586 (1998).
14. Nasseh, I. & Al-Rawi, W. Cone Beam Computed Tomography. *Dent Clin North Am*, **62**, 361–391 https://doi.org/doi:10.1016/j.cden.2018.03.002 (2018).
15. Patel, S. *et al.* Cone beam computed tomography in Endodontics - a review of the literature. *Int Endod J*, **52**, 1138–1152 https://doi.org/doi:10.1111/iej.13115 (2019).
16. Suzuki, T. CT and CT-Dacryocystography for Patient Selection in Nasolacrimal Duct Intubation. *Journal of the Eye*, **32**, 1673–1680 (2015).
17. Tschopp, M., Bornstein, M. M., Sendi, P., Jacobs, R. & Goldblum, D. Dacryocystography using cone beam CT in patients with lacrimal drainage system obstruction. *Ophthalmic Plast Reconstr Surg*, **30**, 486–491 https://doi.org/doi:10.1097/iop.0000000000000154 (2014).
18. Wilhelm, K. E. *et al.* Cone-Beam Computed Tomography (CBCT) dacryocystography for imaging of the nasolacrimal duct system. *Klin Neuroradiol*, **19**, 283–291 https://doi.org/doi:10.1007/s00062-009-9025-9 (2009).
19. Maliborski, A. & Różycki, R. Diagnostic imaging of the nasolacrimal drainage system. Part I. Radiological anatomy of lacrimal pathways. Physiology of tear secretion and tear outflow. *Med Sci Monit*, **20**, 628–638 https://doi.org/doi:10.12659/MSM.890098 (2014).
20. Paulsen, F. [Anatomy and physiology of efferent tear ducts]. *Ophthalmologe*, **105**, 339–345 https://doi.org/doi:10.1007/s00347-008-1735-x (2008).
21. Valencia, M. R. P. *et al.* Lacrimal drainage anatomy in the Japanese population. *Ann Anat*, **223**, 90–99 https://doi.org/doi:10.1016/j.aanat.2019.01.013 (2019).
22. Kim, Y. H., Park, M. G., Kim, G. C., Park, B. S. & Kwak, H. H. Topography of the nasolacrimal duct on the lateral nasal wall in Koreans. *Surg Radiol Anat*, **34**, 249–255 https://doi.org/doi:10.1007/s00276-011-0858-y (2012).
23. Sahni, S., Goyal, R., Gupta, T. & Gupta, A. Surgical Anatomy of Nasolacrimal Duct and Sac in Human Cadavers. *Clinical Rhinology An International Journal*, **7**, 91–95 https://doi.org/doi:10.5005/jp-journals-10013-1205 (2014).

24. Kurihashi, K., Imada, M. & Yamashita, A. Anatomical analysis of the human lacrimal drainage pathway under an operating microscope. *Int Ophthalmol*, **15**, 411–416 https://doi.org/doi:10.1007/bf00137954 (1991).
25. Narioka, J., Matsuda, S. & Ohashi, Y. Correlation between anthropometric facial features and characteristics of nasolacrimal drainage system in connection to false passage. *Clin. Exp. Ophthalmol*, **35**, 651–656 https://doi.org/doi:10.1111/j.1442-9071.2007.01558.x (2007).
26. Park, J. *et al.* The orientation of the lacrimal fossa to the bony nasolacrimal canal: an anatomical study. *Ophthalmic Plast Reconstr Surg*, **28**, 463–466 https://doi.org/doi:10.1097/IOP.0b013e31826463d9 (2012).

Figures

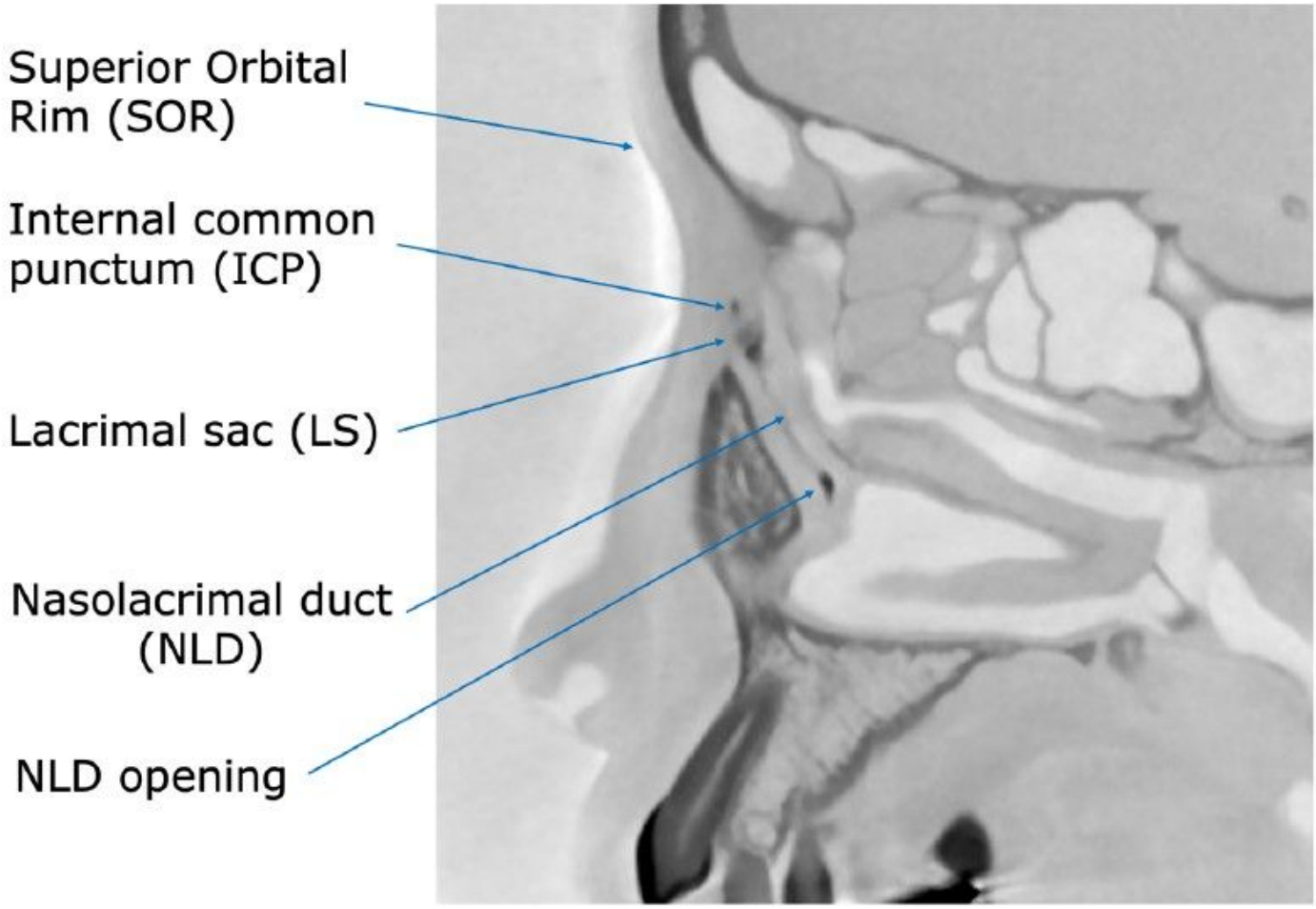

Figure 1

CBCT-DCG sagittal image sectioning the lacrimal duct. The figure shows a dacryocystographic image of the nasolacrimal duct on the right side, from a patient diagnosed with left-sided unilateral primary acquired nasolacrimal duct obstruction. The original image was converted to monochrome to facilitate

observation of the contrast media. Abbreviations: CBCT-DCG, cone-beam computed tomography–dacryocystography.

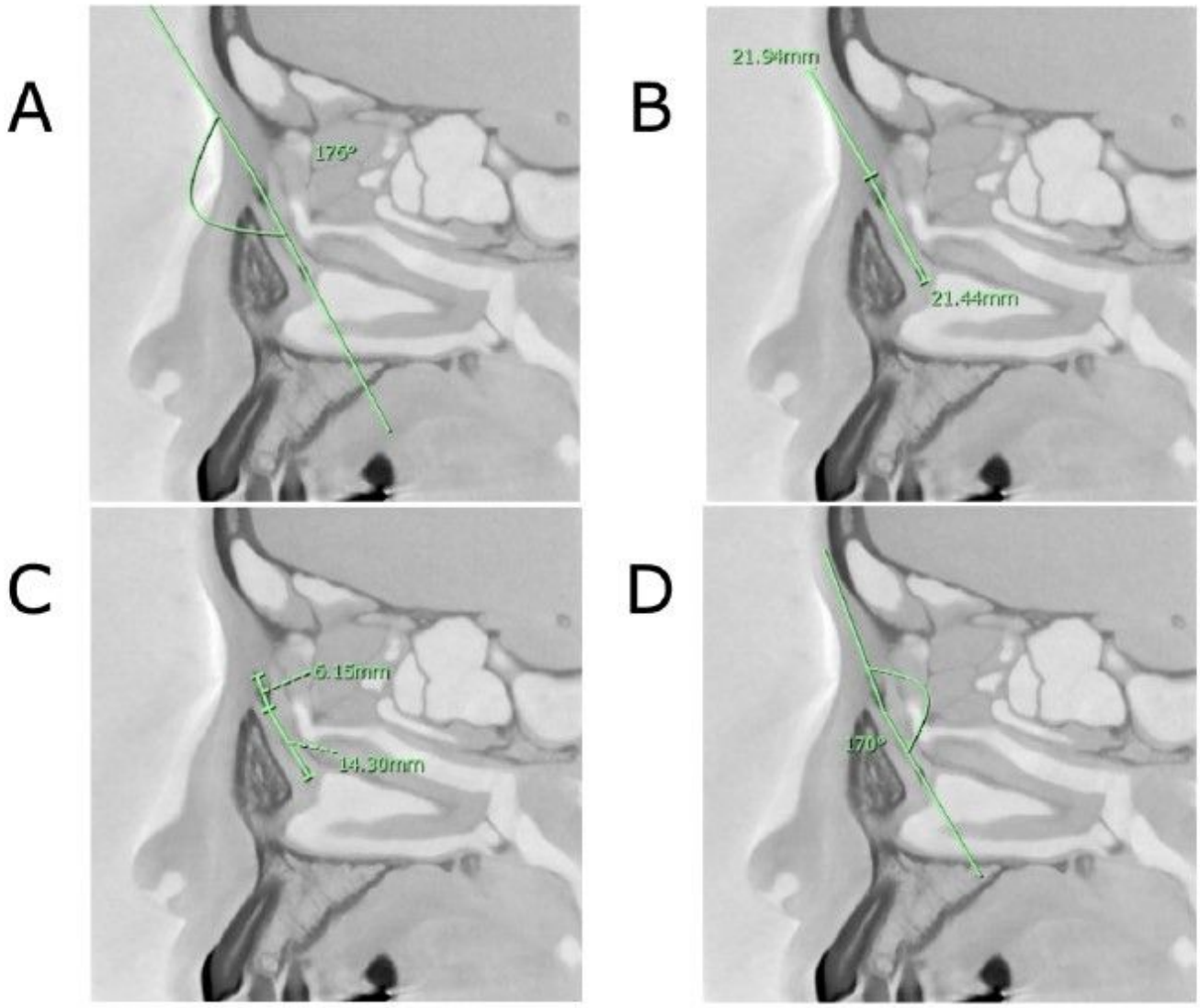

Figure 2

Parameters measured in CBCT-DCG images. (A) the angle formed by SOR–ICP–NLD opening. In this case, the line connecting the ICP– NLD opening was inclined anteriorly at 4° relative to the line connecting the SOR–ICP. (B) The lengths of SOR–ICP and ICP–NLD opening. In this case, the former was 21.94 mm and the latter was 21.44 mm. (C) The length of LS and NLD. In this case, the former was 6.15 mm and the latter was 14.30 mm. (D) The angle formed by LS and NLD. In this case, the long axis of NLD was inclined posteriorly at 10° relative to the LS. Abbreviations: CBCT-DCG, cone-beam computed tomography–dacryocystography; SOR, superior orbital rim; ICP, internal common punctum; NLD, nasolacrimal duct; LS, lacrimal sac.

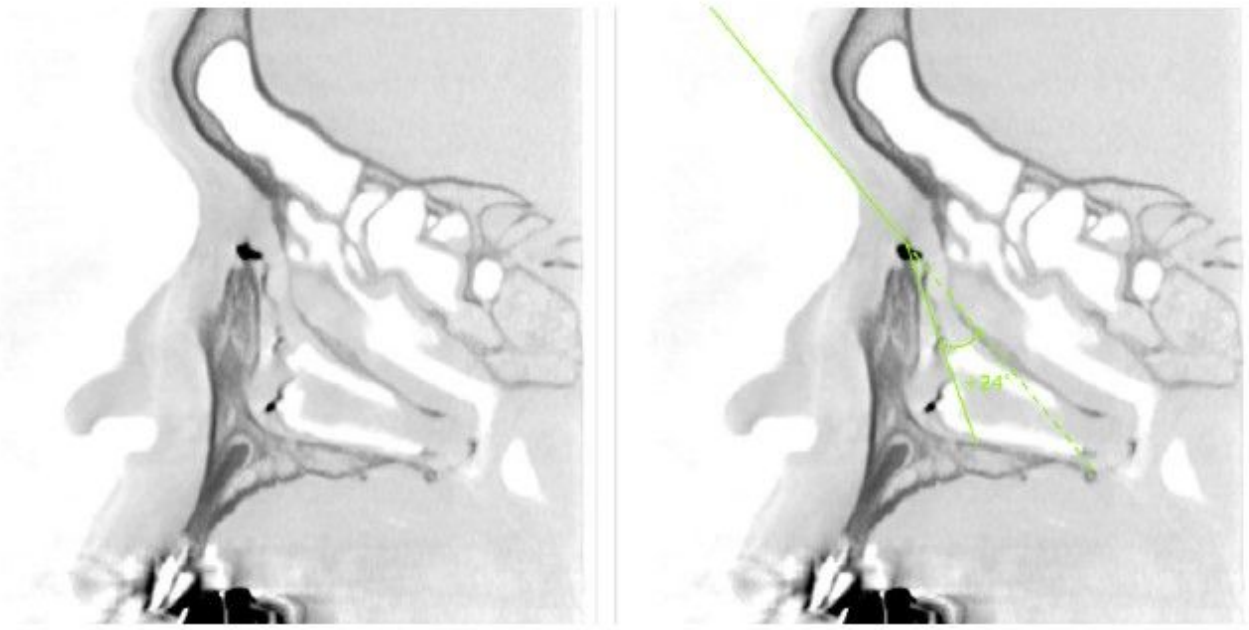

Figure 3

Example of a large SOR–ICP–NLD opening angle. On the left side is the original image. On the right side, a relatively large angle of 24° is seen, due to the elevation of the SOR and the anterior inclination of the NLD. Abbreviations: SOR, superior orbital rim; ICP, internal common punctum; NLD, nasolacrimal duct.

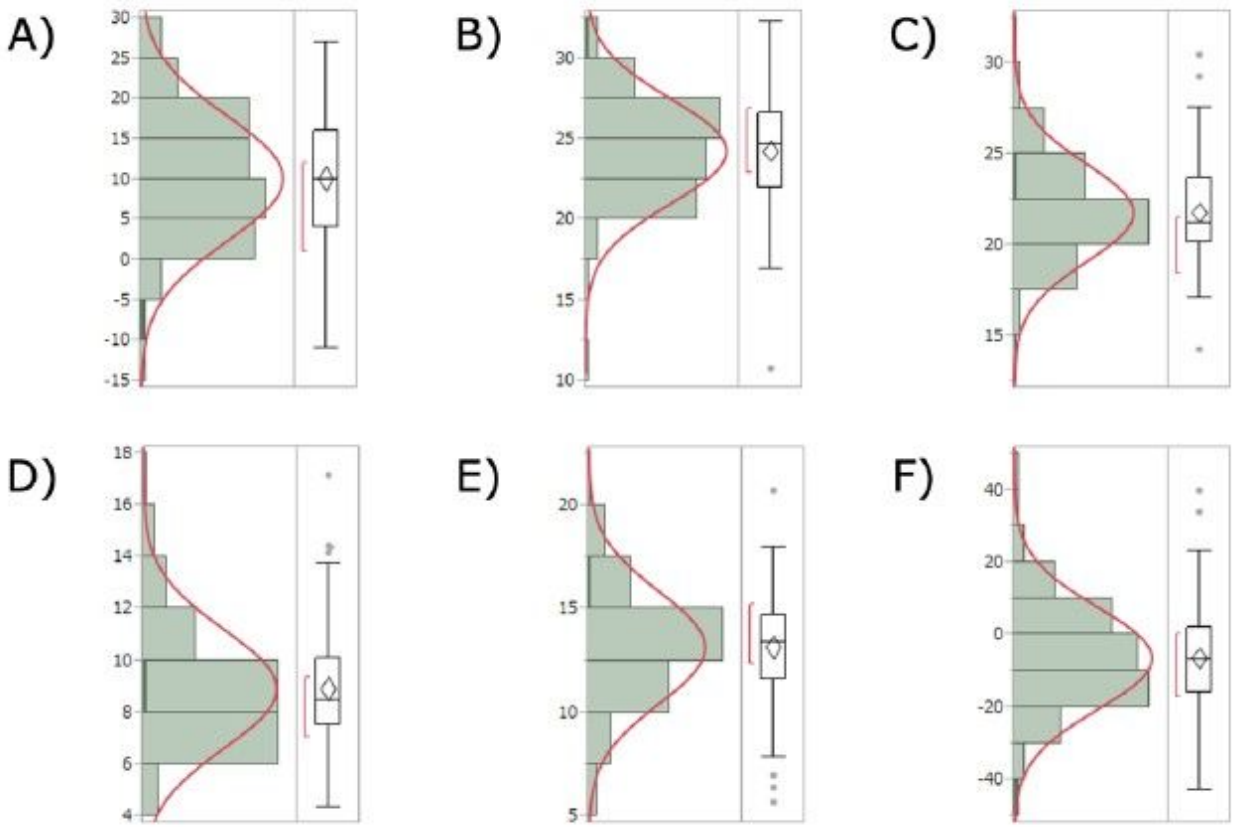

Figure 4

Test results for normal distribution of the measured parameters. (A) SOR–ICP–NLD opening angle: The average angle was 10.7 ± 7.4° (range, −6° to +27°) and followed a normal distribution (p = 0.55). (B) SOR–ICP length: The mean length was 24.3 ± 3.3 mm (range, 10.8–32.2) and did not follow a normal distribution (p = 0.07). (C) ICP–NLD opening length: The mean length was 21.9 ± 2.7 mm (range, 14.2–30.5) and did not follow a normal distribution (p = 0.001). (D) LS length: The mean length was 8.9 ± 2.2 mm (range, 5.4– 17.1) and did not follow a normal distribution (p = 0.078). (E) NLD length: The mean length was 13.3 ± 2.7 mm (range, 5.7–20.7) and followed a normal distribution (p = 0.17). (F) LS–NLD angle: The mean angle was −6.84 ± 13.7° (range, −43° to +34°) and followed a normal distribution (p = 0.28). The p-value was determined by the Shapiro–Wilk test. A p-value of >0.05 indicated a normal distribution. Abbreviations: SOR, superior orbital rim; ICP, interior common punctum; NLD, nasolacrimal duct; LS, lacrimal sac.

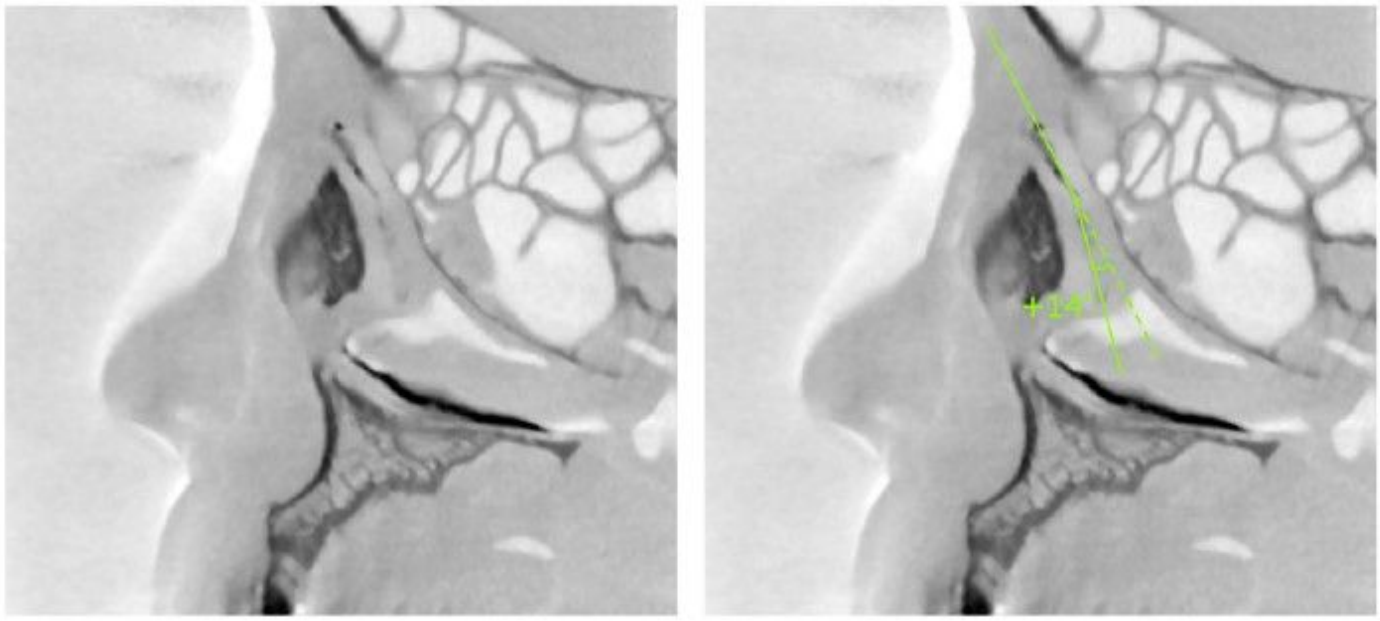

Figure 5

Example in which the NLD is inclined anteriorly to the LS (anterior bending type).On the left is the original image. On the right side, the long axis of the NLD was anteriorly inclined by +14° relative to that of the LS. Abbreviations: NLD, nasolacrimal duct; LS, lacrimal sac.

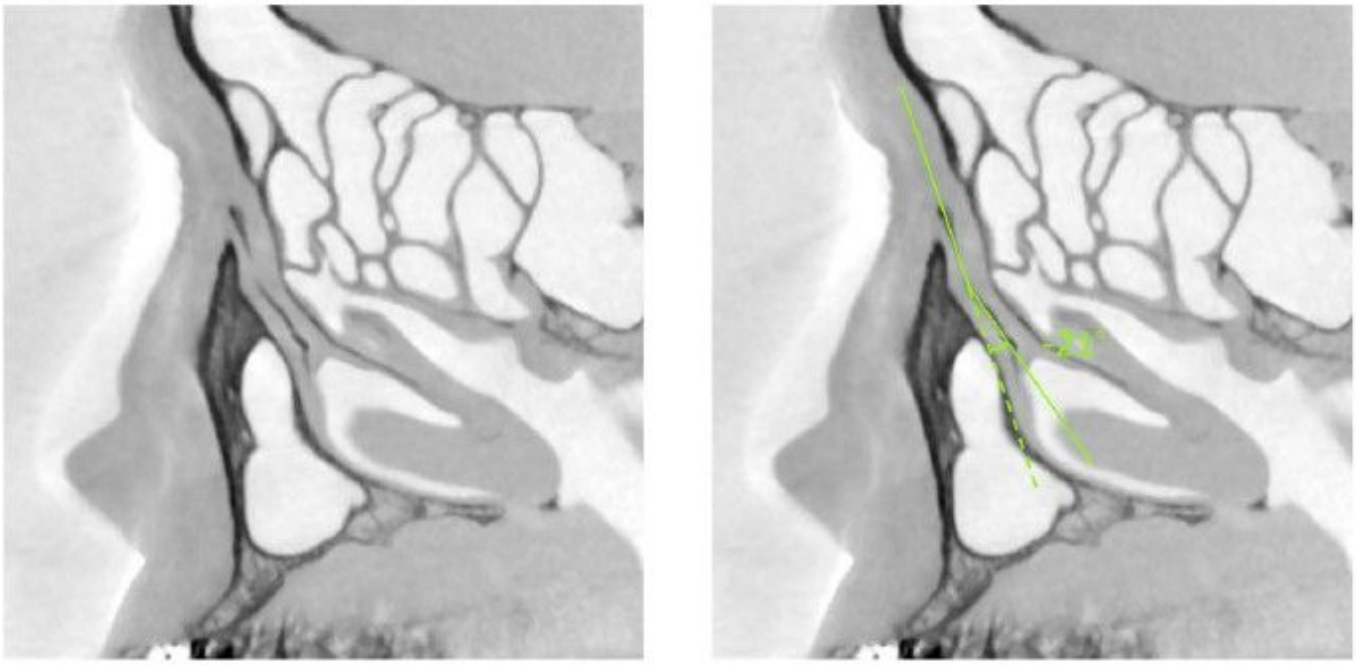

Figure 6

Example in which the NLD is inclined posteriorly to the LS (posterior bending type). On the left is the original image. On the right side, the long axis of the NLD was posteriorly inclined by −21° relative to the LS. Abbreviations: NLD, nasolacrimal duct; LS, lacrimal sac.